

Synthesis and Structure of Yttrium and Lanthanide Bis(phosphinimino)methanides

Michael T. Gamer, Stefanie Dehnen, and Peter W. Roesky*

Institut für Anorganische Chemie, Engesserstrasse 15, D-76128 Karlsruhe, Germany

Received April 10, 2001

Reaction of $K\{CH(PPh_2NSiMe_3)_2\}$ (**1**) with anhydrous yttrium or lanthanide trichlorides leads to $\{[CH(PPh_2NSiMe_3)_2]LnCl_2\}_2$ ($Ln = Y$ (**2a**), Sm (**2b**), Er (**2c**), Dy (**2d**), Yb (**2e**), Lu (**2f**)). The single-crystal X-ray structures of these complexes show that the methine carbon is bound to the lanthanide atom. This is supported by DFT calculations, which show a comparable interaction. Due to the similar ion radii of the lanthanides, the single-crystal X-ray structures of **2a–f** are isostructural. Further reaction of **2** with $KNPh_2$ afforded $\{[CH(PPh_2NSiMe_3)_2]Ln(NPh_2)_2\}$ ($Ln = Y$ (**3a**), Sm (**3b**)). These complexes show in comparison to **2** a similar coordination behavior of the $\{CH(PPh_2NSiMe_3)_2\}^-$ ligand in the solid state and in solution.

Introduction

Metallocenes of organolanthanides¹ have proven to be highly efficient catalysts² for a variety of olefin transformations including hydrogenation,^{3,4} polymerization,⁵ hydroamination,^{6,7} hydrosilylation,⁷ and hydroboration.⁸ Recently, there has been a significant research effort by us and others to substitute the cyclopentadienyl ligand⁹ by anionic nitrogen-based bidentate ligand systems¹⁰ such as benzamidinates¹¹ or aminotroponiminates.¹² Another approach in this area is the use of

P–N ligands such as phosphinimines and phosphinimides.¹³ Our attention is drawn to the phosphinimine $\{CH(PPh_2NSiMe_3)_2\}^-$ as a potential precursor to stable lanthanide complexes. We anticipated that this ligand system may combine the advantages of phosphinimines and amidinates. The central carbon protons of $CH_2(PPh_2NSiMe_3)_2$ are expected to be acidic in analogy with the inorganic ligands $[N(EPPH_2)_2]^-$ ($E = O, S, Se$)^{14–16} and $[CH(EPPH_2)_2]^-$ ($E = O, S, Se$).^{17–19} It was shown that a monoanionic^{20,21} and a dianionic species^{22,23} ($\{CH(PPh_2NSiMe_3)_2\}^-$ and $\{C(PPh_2NSiMe_3)_2\}^{2-}$, respectively) can be generated by deprotonation of the precursor $CH_2(PPh_2-$

(1) Review: (a) Schumann, H.; Meese-Marktscheffel, J. A.; Esser, L. *Chem. Rev.* **1995**, *95*, 865–986. (b) Schaverien, C. J. *Adv. Organomet. Chem.* **1994**, *36*, 283–363. (c) Schumann, H. *Angew. Chem.* **1984**, *96*, 475–493; *Angew. Chem., Int. Ed. Engl.* **1984**, *23*, 474–493.

(2) (a) Edelmann, F. T. *Top. Curr. Chem.* **1996**, *179*, 247–276. (b) Watson, P. L.; Parshall, G. W. *Acc. Chem. Res.* **1985**, *18*, 51–56.

(3) (a) Evans, W. J.; Bloom, I.; Hunter, W. E.; Atwood, J. L. *J. Am. Chem. Soc.* **1983**, *105*, 1401–1403. (b) Jeske, G.; Lauke, H.; Mauermann, H.; Schumann, H.; Marks, T. J. *J. Am. Chem. Soc.* **1985**, *107*, 8111–8118. (c) Conticello, V. P.; Brard, L.; Giardello, M. A.; Tsuji, Y.; Sabat, M.; Stern, C. L.; Marks, T. J. *J. Am. Chem. Soc.* **1992**, *114*, 2761–2762.

(4) Giardello, M.; Conticello, V. P.; Brard, L.; Gagné, M. R.; Marks, T. J. *J. Am. Chem. Soc.* **1994**, *114*, 10241–10254.

(5) (a) Watson, P. L. *J. Am. Chem. Soc.* **1982**, *104*, 337–339. (b) Bunel, E. E.; Burger, B. J.; Bercaw, J. E. *J. Am. Chem. Soc.* **1988**, *110*, 976–981. (c) Coughlin, E. B.; Bercaw, J. E. *J. Am. Chem. Soc.* **1992**, *114*, 7607–7608. (d) Hajela, S.; Bercaw, J. E. *Organometallics* **1994**, *13*, 1147–1154. (e) Jeske, G.; Lauke, H.; Mauermann, H.; Swepston, P. N.; Schumann, H.; Marks, T. J. *J. Am. Chem. Soc.* **1985**, *107*, 8091–8103. (f) Giardello, M. A.; Yamamoto, Y.; Brard, L.; Marks, T. J. *J. Am. Chem. Soc.* **1995**, *117*, 3276–3277.

(6) (a) Gagné, M. R.; Marks, T. J. *J. Am. Chem. Soc.* **1989**, *111*, 4108–4109. (b) Gagné, M. R.; Stern, C. L.; Marks, T. J. *J. Am. Chem. Soc.* **1992**, *114*, 275–294. (c) Li, Y.; Marks, T. J. *J. Am. Chem. Soc.* **1996**, *118*, 9295–9306. (d) Roesky, P. W.; Stern, C. L.; Marks, T. J. *Organometallics* **1997**, *16*, 4705–4711. (e) Li, Y.; Marks, T. J. *J. Am. Chem. Soc.* **1998**, *120*, 1757–1771. (f) Arredondo, V. M.; McDonald, F. E.; Marks, T. J. *J. Am. Chem. Soc.* **1998**, *120*, 4871–4872.

(7) (a) Nolan, S. P.; Porchia, M.; Marks, T. J. *Organometallics* **1991**, *10*, 1450–1457. (b) Sakakura, T.; Lautenschläger, H.-J.; Tanaka, M. *J. Chem. Soc., Chem. Commun.* **1991**, 40–41. (c) Molander, G. A.; Nichols, P. J. *J. Am. Chem. Soc.* **1995**, *117*, 4414–4416. (d) Molander, G. A.; Retsch, W. A. *Organometallics* **1995**, *14*, 4570–4575. (e) Fu, P.-F.; Brard, L.; Li, Y.; Marks, T. J. *J. Am. Chem. Soc.* **1995**, *117*, 7157–7168.

(8) (a) Harrison, K. N.; Marks, T. J. *J. Am. Chem. Soc.* **1992**, *114*, 9220–9221. (b) Bijpost, E. A.; Duchateau, R.; Teuben, J. H. *J. Mol. Catal.* **1995**, *95*, 121–128.

(9) Review: Edelmann, F. T. *Angew. Chem.* **1995**, *107*, 2647–2669; *Angew. Chem., Int. Ed. Engl.* **1995**, *34*, 2466–2488.

(10) Review: (a) Britovsek, G. J. P.; Gibson, V. C.; Wass, D. F. *Angew. Chem.* **1999**, *111*, 448–468; *Angew. Chem., Int. Ed.* **1999**, *38*, 428–447. (b) Kempe, R. *Angew. Chem.* **2000**, *112*, 478–504; *Angew. Chem., Int. Ed.* **2000**, *39*, 468–493.

(11) Review: (a) Edelmann, F. T. *Top. Curr. Chem.* **1996**, *179*, 113–148. (b) Edelmann, F. T. *Coord. Chem. Rev.* **1994**, *137*, 403–481.

(12) (a) Roesky, P. W. *Chem. Ber.* **1997**, *130*, 859–862. (b) Roesky, P. W. *Inorg. Chem.* **1998**, *37*, 4507–4511. (c) Bürgstein, M. R.; Berberich, H.; Roesky, P. W. *Organometallics* **1998**, *17*, 1452–1454. (d) Roesky, P. W.; Bürgstein, M. R. *Inorg. Chem.* **1999**, *38*, 5629–5632. (e) Review: Roesky, P. W. *Chem. Soc. Rev.* **2000**, *29*, 335–345.

(13) Wetzel, T. G.; Dehnen, S.; Roesky, P. W. *Angew. Chem.* **1999**, *111*, 1155–1158; *Angew. Chem., Int. Ed.* **1999**, *38*, 1086–1088.

(14) (a) Bhattacharyya, P.; Woolins, J. D. *Polyhedron* **1995**, *14*, 3367–3388. (b) Bhattacharyya, P.; Slawin, A. M. Z.; Williams, D. J.; Woolins, J. D. *J. Chem. Soc., Dalton Trans.* **1995**, 2489–2495. (c) Bhattacharyya, P.; Novosad, J.; Phillips, J.; Slawin, A. M. Z.; Williams, D. J.; Woolins, J. D. *J. Chem. Soc., Dalton Trans.* **1995**, 3189–3193. (d) Bhattacharyya, P.; Slawin, A. M. Z.; Smith, M. B. *Dalton Trans.* **1998**, 2467–2476.

(15) Geissinger, M.; Magull, J. Z. *Anorg. Allg. Chem.* **1997**, *623*, 755–761.

(16) (a) Perin, C. G.; Ibers, J. A. *Inorg. Chem.* **1999**, *38*, 5478–5483. (b) Perin, C. G.; Ibers, J. A. *Inorg. Chem.* **2000**, *39*, 1222–1226.

(17) Issleib, K.; Abicht, H. P. *J. Prakt. Chem.* **1970**, *312*, 456–465. (18) Baker, P. K.; Harris, S. D.; Durrant, M. C.; Richards, R. *Polyhedron* **1996**, *15*, 3595–3598.

(19) (a) Berry, D. E.; Browning, J.; Dixon, K. R.; Hilts, R. W.; Pidcock, A. *Inorg. Chem.* **1992**, *31*, 1479–1487. (b) Browning, J.; Bushnell, G. W.; Dixon, K. R.; Pidcock, A. *Inorg. Chem.* **1983**, *22*, 2226–2228.

(20) Gamer, M. T.; Roesky, P. W. *Z. Anorg. Allg. Chem.* **2001**, *627*, 877–881.

(21) Kamalesh Babu, R. P.; Aparna, K.; McDonald, R.; Cavell, R. G. *Inorg. Chem.* **2000**, *39*, 4981–4984.

(22) Kasani, A.; Kamalesh Babu, R. P.; McDonald, R.; Cavell, R. G. *Angew. Chem.* **1999**, *111*, 1580; *Angew. Chem., Int. Ed.* **1999**, *38*, 1438.

(23) Ong, C. M.; Stephan, D. W. *J. Am. Chem. Soc.* **1999**, *121*, 2939.

NSiMe₃)₂. The monoanionic species was used as ligands in main group and transition metal chemistry,^{24–27} whereas the dianionic ligand was reported by Cavell and co-workers to form carbene-like complexes with a series of transition metals and samarium.^{27,28}

In this paper we describe the synthesis of a series of lanthanide bis(phosphinimino)methanide dichloride complexes including yttrium, [CH(PPh₂NSiMe₃)₂LnCl₂]₂ (Ln = Y, Sm, Dy, Er, Yb, Lu). Their structures were investigated in solution and in the solid state and rationalized by quantum chemical investigations using density functional theoretical (DFT)²⁹ methods and population analyses. Moreover, a further reaction of the yttrium and the samarium compound to the amido complexes [CH(PPh₂NSiMe₃)₂Ln(NPh₂)₂] (Ln = Y, Sm) is reported.

Experimental Section

General Procedures. All manipulations of air-sensitive materials were performed with the rigorous exclusion of oxygen and moisture in flame-dried Schlenk-type glassware either on a dual-manifold Schlenk line, interfaced to a high-vacuum (10⁻⁴ Torr) line, or in an argon-filled M. Braun glovebox. Ether solvents (tetrahydrofuran and ethyl ether) were predried over Na wire and distilled under nitrogen from Na/K alloy benzophenone ketyl prior to use. Hydrocarbon solvents (toluene and *n*-pentane) were distilled under nitrogen from LiAlH₄. All solvents for vacuum line manipulations were stored in vacuo over LiAlH₄ in resealable flasks. Deuterated solvents were obtained from Aldrich Inc. (all 99 atom % D) and were degassed, dried, and stored in vacuo over Na/K alloy in resealable flasks. NMR spectra were recorded on Bruker AC 250. Chemical shifts are referenced to internal solvent resonances and are reported relative to tetramethylsilane and 85% phosphoric acid (³¹P NMR), respectively. K[CH(PPh₂NSiMe₃)₂]²⁰ was prepared according to literature procedures.

[CH(PPh₂NSiMe₃)₂YCl₂]₂ (**2a**). THF (20 mL) was condensed at -196 °C onto a mixture of 107 mg (0.55 mmol) of YCl₃ and 300 mg (0.5 mmol) of **1**, and the mixture was stirred for 18 h at room temperature. The solution was then filtered and the solvent removed in vacuo. The remaining solid was washed with pentane (3 × 10 mL) and dried in vacuo. Finally, the product was crystallized from hot toluene. Yield: 247 mg (68%). IR (KBr [cm⁻¹]): 1437 (s), 1263 (s), 1245 (s), 1160 (m), 1131 (s), 824 (s), 711 (m), 694 (s), 661 (m), 624 (m), 607 (m), 551 (m), 518 (s), 503 (m). ¹H NMR (THF-*d*₆, 250 MHz, 25 °C):

(24) Imhoff, P.; Guelpen, J. H.; Vrieze, K.; Smeets, W. J. J.; Spek, A. L.; Elsevier, C. J. *Inorg. Chim. Acta* **1995**, *235*, 77–88.

(25) (a) Avis, M. W.; van der Boom, M. E.; Elsevier, C. J.; Smeets, W. J. J.; Spek, A. L. *J. Organomet. Chem.* **1997**, *527*, 263–276. (b) Avis, M. W.; Elsevier, C. J.; Ernsting, J. M.; Vrieze, K.; Veldman, N.; Spek, A. L.; Katti, K. V.; Barnes, C. L. *Organometallics* **1996**, *15*, 2376–2392. (c) Avis, M. W.; Vrieze, K.; Kooijman, H.; Veldman, N.; Spek, A. L.; Elsevier, C. J. *Inorg. Chem.* **1995**, *34*, 4092–4105. (d) Imhoff, P.; van Asselt, R.; Ernsting, J. M.; Vrieze, K.; Elsevier, C. J.; Smeets, W. J. J.; Spek, A. L.; Kentgens, A. P. M. *Organometallics* **1993**, *12*, 1523–1536.

(26) Ong, C. M.; McKarns, P.; Stephan, D. W. *Organometallics* **1999**, *18*, 4197–4208.

(27) (a) Kasani, A.; Kamalesh Babu, R. P.; McDonald, R.; Cavell, R. G. *Organometallics* **1999**, *18*, 3775–3777. (b) Aparna, K.; McDonald, R.; Ferguson, M.; Cavell, R. G. *Organometallics* **1999**, *18*, 4241–4243.

(28) (a) Kamalesh Babu, R. P.; McDonald, R.; Decker, S. A.; Klobukowski, M.; Cavell, R. G. *Organometallics* **1999**, *18*, 4226–4229. (b) Cavell, R. G.; Kamalesh Babu, R. P.; Kasani, A.; McDonald, R. *J. Am. Chem. Soc.* **1999**, *121*, 5805–5806. (c) Kamalesh Babu, R. P.; McDonald, R.; Cavell, R. G. *Chem. Commun.* **2000**, 481–482. (d) Kasani, A.; Ferguson, M.; Cavell, R. G. *J. Am. Chem. Soc.* **2000**, *112*, 726–727.

(29) (a) Parr, R. G.; Yang, W. *Density Functional Theory of Atoms and Molecules*; Oxford University Press: New York, 1988. (b) Ziegler, T. *Chem. Rev.* **1991**, *91*, 651–667.

δ 0.14 (s, 36H, SiMe₃), 1.93 (dt, 2H, CH, ²J(H,P) = 1.94 Hz, ²J(H,Y) = 0.92 Hz), 6.88–7.05 (m, 8H, Ph), 7.07–7.27 (m, 12H, Ph), 7.36–7.55 (m, 12H, Ph), 7.80–8.08 (br, 8H, Ph). ¹³C{¹H} NMR (THF-*d*₆, 62.9 MHz, 25 °C): δ 4.3 (SiMe₃), 17.6 (dt, CH, ¹J(C,P) = 89.1 Hz, ¹J(C,Y) = 3.6 Hz), 128.6 (d, Ph), 131.0 (Ph), 132.3 (m, Ph), 132.6 (m, Ph). ²⁹Si NMR (THF-*d*₆, 49.7 MHz, 25 °C): δ -1.6. ³¹P{¹H} NMR (THF-*d*₆, 101.3 MHz, 25 °C): δ 20.4 (d, ²J(P,Y) = 5.8 Hz). C₆₂H₇₈Cl₄N₄P₄Si₄Y₂ (1435.18): calcd C 51.89, H 5.48, N 3.90; found C 51.57, H 5.40, N 3.78.

[CH(PPh₂NSiMe₃)₂LnCl₂]₂ (Ln = Sm (**2b**), Dy (**2c**), Er (**2d**)). THF (20 mL) was condensed at -196 °C onto a mixture of 1.10 mmol LnCl₃ and 600 mg (1.0 mmol) of **1**, and the mixture was stirred for 18 h at room temperature. The solvent was then evaporated in vacuo and toluene condensed onto the mixture. The mixture was shortly refluxed and then filtered and the solvent taken off in vacuo. The remaining solid was washed with pentane (3 × 10 mL) and dried in vacuo. Finally, the product was crystallized from hot toluene.

2b (Ln = Sm): Yield 535 mg (69%). IR (KBr [cm⁻¹]): 1437 (s), 1262 (s), 1242 (s), 1170 (m), 1108 (s), 825 (s), 742 (m), 692 (s), 663 (m), 605 (m), 554 (m), 519 (m), 504 (m). ¹H NMR (THF-*d*₆, 250 MHz, 25 °C): δ 0.32 (br, 36H, SiMe₃), 2.61 (br, 2H, CH), 6.80–7.05 (br, 8H, Ph), 7.05–7.50 (br, 24H, Ph), 7.60–7.85 (br, 8H, Ph). ¹³C{¹H} NMR (THF-*d*₆, 62.9 MHz, 25 °C): δ 4.2 (SiMe₃), 21.4 (br, CH), 128.7 (br, Ph), 131.1 (br, Ph), 132.6 (br, Ph), 138.3 (br, Ph). ³¹P{¹H} NMR (THF-*d*₆, 101.3 MHz, 25 °C): δ 31.2. C₆₂H₇₈Cl₄N₄P₄Si₄Sm₂ (1558.10): calcd C 47.79, H 5.05, N 3.60; found C 47.66, H 4.98, N 3.52.

2c (Ln = Dy): Yield 324 mg (41%). IR (KBr [cm⁻¹]): 1437 (s), 1261 (s), 1246 (s), 1107 (m), 847 (s), 744 (m), 711 (m), 693 (s), 661 (m), 551 (m), 517 (m). EI/MS (70 eV) *m/z* (%): 791 ([M/2]⁺, rel int. 17), 776 ([M/2 - Me]⁺, 12), 543 ([C₃₀H₃₆N₂P₂Si₂]⁺, 97), 471 ([C₂₈H₃₁NP₂Si]⁺, 100), 456 ([C₂₇H₂₈NP₂Si]⁺, 90). C₆₂H₇₈Cl₄N₄P₄Si₄Dy₂ (1582.38): calcd C 47.06, H 4.97, N 3.54; found C 47.01, H 4.82, N 3.45.

2d (Ln = Er): Yield 270 mg (34%). IR (KBr [cm⁻¹]): 1437 (s), 1262 (s), 1247 (s), 1125 (s), 828 (s), 743 (m), 711 (m), 693 (s), 661 (m), 624 (m), 551 (m), 517 (s), 504 (m). EI/MS (70 eV) *m/z* (%): 795 ([M/2]⁺, rel int. 3), 780 ([M/2 - Me]⁺, 2), 558 ([C₃₁H₃₉N₂P₂Si₂]⁺, 57), 543 ([C₃₀H₃₆N₂P₂Si₂]⁺, 100), 471 ([C₂₈H₃₁NP₂Si]⁺, 92). C₆₂H₇₈Cl₄N₄P₄Si₄Er₂ (1591.90): calcd C 46.78, H 4.94, N 3.52; found C 46.46, H 5.25, N 3.18.

[CH(PPh₂NSiMe₃)₂LnCl₂]₂ (Ln = Yb (**2e**), Lu (**2f**)). THF (20 mL) was condensed at -196 °C onto a mixture of 0.44 mmol LnCl₃ and 241 mg (0.40 mmol) of **1**, and the mixture was stirred for 18 h at room temperature. Then, the solution was filtered and the solvent removed. The remaining solid was washed with pentane (3 × 10 mL) and dried in vacuo. Finally, the product was crystallized from hot toluene.

2e (Ln = Yb): Yield 205 mg (64%). IR (KBr [cm⁻¹]): 1437 (s), 1263 (s), 1246 (s), 1160 (m), 1131 (s), 824 (s), 711 (m), 694 (s), 661 (m), 624 (m), 607 (m), 551 (m), 518 (s), 503 (m). EI/MS (70 eV) *m/z* (%): 801 ([M/2]⁺, rel int 0.8), 786 ([M/2 - Me]⁺, 2), 558 ([C₃₁H₃₉N₂P₂Si₂]⁺, 34), 543 ([C₃₀H₃₆P₂Si₂]⁺, 100). C₆₂H₇₈Cl₄N₄P₄Si₄Yb₂ (1603.46): calcd C 46.44, H 4.90, N 3.49; found C 46.27, H 5.19, N 3.15.

2f (Ln = Lu): Yield 189 mg (59%). ¹H NMR (THF-*d*₆, 250 MHz, 25 °C): δ 0.14 (s, 36H, SiMe₃), 1.97 (t, 2H, CH, ²J(H,P) = 1.95 Hz), 6.90–7.04 (br, 8H, Ph), 7.11–7.26 (m, 12H, Ph), 7.36–7.54 (m, 12H, Ph), 7.90–8.06 (m, 8H, Ph). ¹³C{¹H} NMR (THF-*d*₆, 62.9 MHz, 25 °C): δ 4.5 (SiMe₃), 17.6 (t, CH, ¹J(H,C) = 87.5 Hz), 128.7 (d, Ph), 132.0 (d, Ph), 132.6 (d, Ph), 138.0 (d, Ph). ²⁹Si NMR (THF-*d*₆, 49.7 MHz, 25 °C): δ -0.5. ³¹P{¹H} NMR (THF-*d*₆, 101.3 MHz, 25 °C): δ 20.5. C₆₂H₇₈Cl₄N₄P₄Si₄Lu₂ (1607.32): calcd C 46.44, H 4.90, N 3.49; found C 46.68, H 5.12, N 3.11.

[CH(PPh₂NSiMe₃)₂Ln(NPh₂)₂] (Ln = Y (**3a**), Sm (**3b**)). THF (20 mL) was condensed at -196 °C onto a mixture of 0.50 mmol of **2** and 207 mg (1.0 mmol) of KNPh₂, and the mixture was stirred for 18 h at room temperature. The solvent was then evaporated in vacuo and toluene (20 mL) condensed onto

Table 1. Crystallographic Details of $[\{\text{CH}(\text{PPh}_2\text{NSiMe}_3)_2\}\text{LnCl}_2]_2$ (2a–f**)^a**

	2a ·(2 toluene)	2b ·(2 toluene)	2c ·(2 toluene)
formula	C ₇₆ H ₉₄ Cl ₄ N ₄ P ₄ Si ₄ Y ₂	C ₇₆ H ₉₄ Cl ₄ N ₄ P ₄ Si ₄ Sm ₂	C ₇₆ H ₉₄ Cl ₄ N ₄ P ₄ Si ₄ Dy ₂
fw	1619.42	1742.30	1766.60
space group	<i>P</i> $\bar{1}$ (No. 2)	<i>P</i> $\bar{1}$ (No. 2)	<i>P</i> $\bar{1}$ (No. 2)
<i>a</i> , Å	11.6542(5)	11.579(8)	11.5748(9)
<i>b</i> , Å	14.3959(5)	14.371(8)	14.3016(12)
<i>c</i> , Å	14.7218(7)	14.751(13)	14.6348(12)
α , deg	63.758(3)	63.37(8)	63.715(9)
β , deg	73.465(4)	73.36(9)	73.456(9)
γ , deg	74.811(4)	74.89(7)	74.816(9)
<i>V</i> , Å ³	2096.9(2)	2077(3)	2056.0(3)
<i>Z</i>	1	1	1
density (g/cm ³)	1.282	1.393	1.427
radiation	Mo K α ($\lambda = 0.71073$ Å)	Mo K α ($\lambda = 0.71073$ Å)	Ag K α ($\lambda = 0.56087$ Å)
μ , mm ⁻¹	1.679	1.705	1.427
abs corr	ψ -scan	none	none
no. of reflns collected	7429	18 290	19 253
no. of unique reflns	7429	7456 [<i>R</i> _{int} = 0.0689]	9021 [<i>R</i> _{int} = 0.0291]
no. of obsd reflns	6344	6863	7885
no. of data; params	7418; 390	7456; 378	9021, 378
<i>R</i> 1; ^b <i>wR</i> 2 ^c	0.0492; 0.1529	0.0407; 0.1250	0.0357; 0.1003

	2d ·(2 toluene)	2e ·(2 toluene)	2f ·(2 toluene)
formula	C ₇₆ H ₉₄ Cl ₄ N ₄ P ₄ Si ₄ Er ₂	C ₇₆ H ₉₄ Cl ₄ N ₄ P ₄ Si ₄ Yb ₂	C ₇₆ H ₉₄ Cl ₄ N ₄ P ₄ Si ₄ Lu ₂
fw	1776.12	1787.68	1791.54
space group	<i>P</i> $\bar{1}$ (No. 2)	<i>P</i> $\bar{1}$ (No. 2)	<i>P</i> $\bar{1}$ (No. 2)
<i>a</i> , Å	11.663(2)	11.654(3)	11.6426(2)
<i>b</i> , Å	14.377(2)	14.340(2)	14.33340(14)
<i>c</i> , Å	14.7310(12)	14.687(3)	14.67890(13)
α , deg	63.84(4)	64.000(3)	64.048(8)
β , deg	73.49(2)	73.45(2)	73.538(10)
γ , deg	74.750(15)	73.45(2)	74.842(15)
<i>V</i> , Å ³	2098.2(5)	2088.2(7)	2085.27(4)
<i>Z</i>	1	1	1
density (g/cm ³)	1.406	1.422	1.427
radiation	Mo K α ($\lambda = 0.71073$ Å)	Mo K α ($\lambda = 0.71073$ Å)	Mo K α ($\lambda = 0.71073$ Å)
μ , mm ⁻¹	2.288	2.529	2.657
abs corr	ψ -scan	ψ -scan	ψ -scan
no. of reflns collected	6817	8244	7954
no. of unique reflns	6816	7373 [<i>R</i> _{int} = 0.0498]	7407 [<i>R</i> _{int} = 0.0651]
no. of obsd reflns	5625	6451	6500
no. of data; params	6816; 378	7373; 378	7407; 378
<i>R</i> 1; ^b <i>wR</i> 2 ^c	0.0490; 0.1422	0.0374; 0.1081	0.0376; 0.1103

^a All data collected at 203 K. ^b *R*1 = $\sum |F_o| - |F_c| / \sum |F_o|$. ^c *wR*2 = $\{\sum [w(F_o^2 - F_c^2)^2] / \sum [w(F_o^2)]\}^{1/2}$.

the mixture. The solution was filtered and concentrated until a precipitate is formed (about 3 mL of solution). The precipitate was dissolved in boiling toluene. Crystals were obtained after 1 day.

3a (Ln = Y): Yield 100 mg (22%). ¹H NMR (C₆D₆, 250 MHz, 25 °C): δ -0.06 (s, 18H, SiMe₃), 2.20 (t, 1H, CH, ²*J*(H,P) = 4.9 Hz), 6.70–7.75 (m, 40H, Ph). ²⁹Si NMR (C₆D₆, 49.7 MHz, 25 °C): δ -1.0. ³¹P{¹H} NMR (C₆D₆, 101.3 MHz, 25 °C): δ 22.1 (d, ²*J*(P,Y) = 6.2 Hz). EI/MS (70 eV) *m/z* (%): 982 ([M]⁺, rel int 0.1), 814 ([M - NPh₂]⁺, 20), 735 ([M - (NPh₂)PhH]⁺, 100), 543 ([C₃₀H₃₆N₂P₂Si₂]⁺, 76), 169 ([NPh₂]⁺, 63). C₅₅H₅₉N₄P₂-Si₂Y (983.12): calcd C 67.19, H 6.05, N 5.70; found C 66.92, H 5.95, N 5.80.

3b (Ln = Sm): Yield 220 mg (42%). ¹H NMR (C₆D₆, 250 MHz, 25 °C): δ -0.76 (s, 18H, SiMe₃), 4.98 (br, 1H, CH), 6.60–7.20 (m, 40H, Ph). ²⁹Si NMR (C₆D₆, 49.7 MHz, 25 °C): δ -1.0. ³¹P{¹H} NMR (C₆D₆, 101.3 MHz, 25 °C): δ 33.4. EI/MS (70 eV) *m/z* (%): 1045 ([M]⁺, rel int 0.1), 877 ([M - NPh₂]⁺, 5), 798 ([M - (NPh₂)PhH]⁺, 40), 543 ([C₃₀H₃₆N₂P₂Si₂]⁺, 76), 169 ([NPh₂]⁺, 100). C₅₅H₅₉N₄P₂Si₂Sm (1044.58): calcd C 63.24, H 5.69, N 5.36; found C 63.01, H 5.37, N 5.57.

X-ray Crystallographic Studies of 2a–f and 3a. Crystals of **2a–f** and **3a** were grown from hot toluene. A suitable crystal was covered in mineral oil (Aldrich) and mounted onto a glass fiber. The crystal was transferred directly to the -73 °C cold

N₂ stream of a Stoe IPDS or a Stoe STADI 4 diffractometer. Subsequent computations were carried out on a Intel Pentium III PC.

All structures were solved by the Patterson method (SHELXS-97³⁰). The remaining non-hydrogen atoms were located from successive difference Fourier map calculations. The refinements were carried out by using full-matrix least-squares techniques on *F*, minimizing the function $(F_o - F_c)^2$, where the weight is defined as $4F_o^2/2(F_o^2)$ and *F*_o and *F*_c are the observed and calculated structure factor amplitudes using the program SHELXL-97.³¹ In the final cycles of each refinement, all non-hydrogen atoms except the toluene molecules were assigned anisotropic temperature factors. Carbon-bound hydrogen atom positions were calculated and allowed to ride on the carbon to which they are bonded assuming a C–H bond length of 0.95 Å. The hydrogen atom contributions were calculated, but not refined. The final values of refinement parameters are given in Tables 1 and 3. The locations of the largest peaks in the final difference Fourier map calculation as well as the magnitude of the residual electron densities in each case were of no chemical significance. Positional parameters, hydrogen atom parameters, thermal parameters, and

(30) Sheldrick, G. M. *SHELXS-97, Program of Crystal Structure Solution*; University of Göttingen: Germany, 1997.

(31) Sheldrick, G. M. *SHELXL-97, Program of Crystal Structure Refinement*; University of Göttingen, Germany, 1997.

Table 2. Selected Bond Lengths (Å) and Angles (deg) of [$\{\text{CH}(\text{PPh}_2\text{NSiMe}_3)_2\}\text{LnCl}_2\}_2$ (2a–f**)**

	2a	2b	2c	2d	2e	2f
Bond Lengths (Å)						
Ln–C1	2.642(4)	2.720(5)	2.641(3)	2.625(7)	2.607(5)	2.596(5)
Ln–N1	2.335(3)	2.391(4)	2.330(3)	2.327(6)	2.301(4)	2.291(4)
Ln–N2	2.357(3)	2.400(4)	2.344(3)	2.344(6)	2.317(4)	2.313(4)
Ln–Cl1	2.5484(13)	2.614(3)	2.5452(11)	2.541(3)	2.511(2)	2.500(2)
Ln–Cl2	2.7170(11)	2.777(2)	2.7077(10)	2.699(2)	2.677(2)	2.6667(15)
Ln–Cl2'	2.6826(12)	2.732(2)	2.6743(10)	2.668(2)	2.643(2)	2.6309(15)
P1–N1	1.608(3)	1.607(4)	1.598(3)	1.616(6)	1.611(4)	1.607(4)
P2–N2	1.606(3)	1.611(4)	1.598(3)	1.610(6)	1.609(4)	1.606(4)
P1–C1	1.751(4)	1.751(4)	1.741(3)	1.749(7)	1.756(5)	1.761(5)
P2–C1	1.749(4)	1.734(4)	1.737(4)	1.743(7)	1.747(5)	1.740(5)
Bond Angles (deg)						
Cl2–Ln–Cl2'	77.51(4)	76.99(6)	77.46(3)	77.63(6)	78.00(5)	77.96(5)
Cl1–Ln–Cl2	98.38(5)	99.40(10)	100.04(4)	98.28(9)	97.48(6)	97.57(6)
N1–Ln–Cl1	99.32(9)	100.45(13)	99.38(8)	99.0(2)	99.07(11)	99.01(12)
N1–Ln–Cl2	160.41(9)	158.35(9)	160.12(8)	160.84(15)	161.48(11)	161.51(12)
N2–Ln–Cl1	105.17(9)	107.94(12)	105.47(7)	104.56(15)	104.18(12)	103.74(11)
N2–Ln–Cl2	86.91(9)	86.91(10)	86.90(7)	87.11(14)	86.72(11)	86.80(11)
N1–Ln–N2	96.47(12)	95.09(12)	96.18(11)	96.6(2)	97.21(15)	97.1(2)
Ln–Cl2–Ln'	102.49(4)	103.01(4)	102.54(3)	102.37(6)	102.00(1)	102.04(1)
P1–C1–P2	124.5(2)	124.7(2)	124.5(2)	124.7(4)	124.1(3)	123.8(3)
P1–N1–Ln	99.7(2)	101.7(2)	100.89(14)	100.2(3)	100.2(2)	100.5(2)
P2–N2–Ln	99.7(2)	100.5(2)	99.94(14)	99.6(3)	99.5(2)	99.2(2)

Table 3. Crystallographic Details of [$\{\text{CH}(\text{PPh}_2\text{NSiMe}_3)_2\}\text{Y}(\text{NPh}_2)_2$] (3a**)^a**

	3a (toluene)
formula	C ₆₂ H ₆₇ N ₄ P ₂ Si ₂ Y
fw	1075.23
space group	P1 (No. 2)
a, Å	12.3776(9)
b, Å	12.6813(9)
c, Å	20.9540(13)
α, deg	90.128(8)
β, deg	99.638(8)
γ, deg	117.207(7)
V, Å ³	2872.2(3)
Z	2
density (g/cm ³)	1.243
radiation	Mo Kα (λ = 0.71073 Å)
μ, mm ⁻¹	1.154
abs corr	ψ-scan
no. of reflns collected	10 766
no. of unique reflns	10 174 [R _{int} = 0.0684]
no. of obsd reflns	8678
no. of data; params	10 174; 624
R1; ^b wR2 ^c	0.0476; 0.1338

^a All data collected at 203 K. ^b R1 = $\sum ||F_o| - |F_c|| / \sum |F_o|$. ^c wR2 = $[\sum [w(F_o^2 - F_c^2)^2] / \sum [w(F_o^2)^2]]^{1/2}$.

bond distances and angles have been deposited as Supporting Information. Crystallographic data (excluding structure factors) for the structures reported in this paper have been deposited with the Cambridge Crystallographic Data Centre as supplementary publication no. CCDC-164392-164398. Copies of the data can be obtained free of charge on application to CCDC, 12 Union Road, Cambridge CB21EZ, U.K. (fax: (+44)1223-336-033; email: deposit@ccdc.cam.ac.uk).

Methods of the Theoretical Investigations. It has been formerly proved that density functional theoretical (DFT)²⁹ calculations are suitable for the theoretical investigation of yttrium and lanthanide systems.¹³ The program system Turbomole³² was employed to carry out the DFT investigations using the efficient Ridft program³³ with the Becke–Perdew (B–P) functional³⁴ and the gridsize m3. The Ridft program has

been developed based on the DFT program,³⁵ approximating the coulomb part of the two-electron interactions. Basis sets were of SV(P) quality (SV(P) = split valence plus polarization for all non-hydrogen atoms, split valence for hydrogen atoms).³⁶ The Y atom was treated with the effective core potential ECP-28,³⁷ which serves as approximation for 28 inner electrons considering relativistic effects. The shared electron numbers (SEN) were calculated pursuant to a method based on occupation numbers that was reported by Ehrhardt and Ahlrichs.³⁸ The calculation was performed by means of the program Moloch equally implemented in Turbomole.

Results and Discussion

Lanthanide Chloride Complexes. Transmetalation of the potassium methanide complex K{CH(PPh₂NSiMe₃)₂} (**1**) with anhydrous yttrium or lanthanide trichlorides in a 1:1.1 molar ratio in THF followed by crystallization from hot toluene afforded the corresponding yttrium and lanthanide complexes [$\{\text{CH}(\text{PPh}_2\text{NSiMe}_3)_2\}\text{LnCl}_2\}_2$ (Ln = Y (**2a**), Sm (**2b**), Er (**2c**), Dy (**2d**), Yb (**2e**), Lu (**2f**)) as large crystals in good yields (eq 1).³⁹ Whereas the complexes **2a**, **2e**, and **2f** were already obtained at room temperature, due to a decreased solubility of the lighter lanthanide trichlorides for **2b**, **2c**, and **2d**, an additional heating of the reaction mixture was necessary to ensure a quantitative reaction. The potassium reagent **1**, which was described earlier,²⁰ was used as starting material to avoid coordination of lighter alkali halides such as lithium chloride. The new complexes have been characterized by standard analytical/spectroscopic techniques, and the solid-state structures of all six compounds were established by single-crystal X-ray diffraction.

(34) (a) Becke, A. D. *Phys. Rev. A* **1988**, *38*, 3098–3109. (b) Vosko, S. H.; Wilk, L.; Nusair, M. *Can. J. Phys.* **1980**, *58*, 1200–1205. (c) Perdew, J. P. *Phys. Rev. B* **1986**, *33*, 8822–8837.

(35) Treutler, O.; Ahlrichs, R. *J. Chem. Phys.* **1995**, *102*, 346–354. (36) Schäfer, A.; Horn, H.; Ahlrichs, R. *J. Chem. Phys.* **1992**, *97*, 2571–2577.

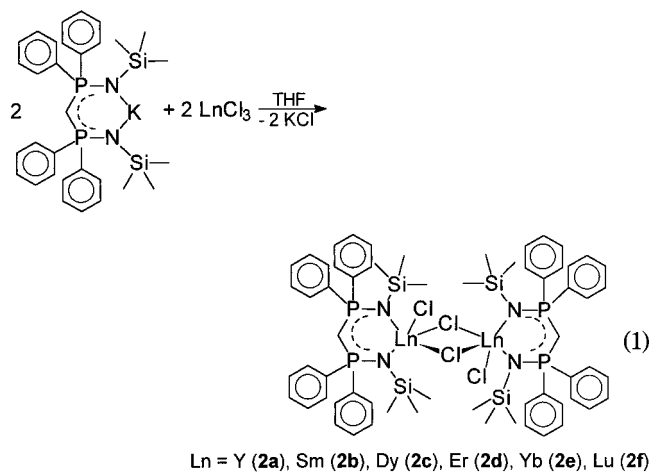
(37) Dolg, M.; Stoll, H.; Savin, A.; Preuss, H. *Theor. Chim. Acta* **1989**, *75*, 173–194.

(38) Ehrhardt, C.; Ahlrichs, R. *Theor. Chim. Acta* **1985**, *68*, 231–245.

(39) The bonding situation in the drawings of the ligand system in eqs 1 and 2 is simplified for clarity.

(32) Ahlrichs, R.; Bär, M.; Häser, M.; Horn, H.; Kölmel, C. *Chem. Phys. Lett.* **1995**, *242*, 652–657.

(33) (a) Eichkorn, K.; Treutler, O.; Öhm, H.; Häser, M.; Ahlrichs, R. *Chem. Phys. Lett.* **1995**, *242*, 652–660. (b) Eichkorn, K.; Weigend, F.; Treutler, O.; Ahlrichs, R. *Theor. Chim. Acta* **1997**, *97*, 119–124.



The ^1H NMR spectra of the diamagnetic compounds **2a-f** show a slight downfield shift of the methine proton (δ 1.93 (**2a**), 1.97 (**2f**)) compared to **1** (δ 1.58). The $^2J(\text{H,P})$ coupling constant of the methine proton (e.g., **2f** $^2J(\text{H,P}) = 1.9$ Hz) is smaller than that of **1** (2.8 Hz). Furthermore, for **2a** a small splitting of the signals in the ^1H and ^{13}C NMR spectra is seen for the methine group. We suggest that this splitting is caused by a $^2J(\text{H,Y})$ coupling (0.92 Hz) and a $^1J(\text{C,Y})$ coupling (3.6 Hz). The coupling constants are much smaller than the ones observed for Y-CH₂SiMe₃ groups ([Y(CH₂SiMe₃)₃(THF)₂]: $^1J(\text{C,Y}) = 35.7$ Hz; $^2J(\text{H,Y}) = 2.3$ Hz),⁴⁰ but the $^1J(\text{C,Y})$ coupling is in the range of a ($\eta^8\text{-C}_8\text{H}_8$)Y group ([($\eta^8\text{-C}_8\text{H}_8$)Y{Ph₂P(NSiMe₃)₂}(THF)]: $^1J(\text{C,Y}) = 2$ Hz).⁴¹ The small coupling constants observed for **2a** may be caused by the very long Y-C_{methine} bond length (see below). The observed couplings suggest a rigid structure of **2** in solution.

The signals of the phenyl protons are broadened in the ^1H NMR spectrum. Complexes **2a-f** each show a sharp signal in the $^{31}\text{P}\{^1\text{H}\}$ NMR spectra (δ 20.4 (**2a**), 20.5 (**2f**)) shifted downfield by about 10 ppm relative to **1** (δ 13.0), showing that the phosphorus atoms in each case are chemically equivalent in solution. In the $^{31}\text{P}\{^1\text{H}\}$ NMR spectrum of **2a** a $^2J(\text{P,Y})$ coupling of 5.8 Hz is observed. Also for **2b** ^1H , ^{13}C , and ^{31}P NMR spectra were obtained, which are quantitatively comparable to those of **2a-f**. Nevertheless, due to the influence of the paramagnetic samarium center, the observed chemical shifts are significantly different, e.g., $\delta(^{31}\text{P}\{^1\text{H}\})$ 31.2. The solid-state IR spectra of **2** are quite similar to each other. They show an intense $\nu_{\text{P=N}}$ absorption around 1245 cm⁻¹.

The structures of **2a-f** were confirmed by single-crystal X-ray diffraction in the solid state. Data collection parameters and selected bond lengths and angles are given in Tables 1 and 2. Due to the similar ion radii of the lanthanides, the single-crystal X-ray structures of **2a-f** are isostructural. As a representative example, the structure of **2f** is shown in Figure 1. In this series, samarium was the largest center metal for which single crystals could be obtained. Attempts to obtain crystals from reactions of neodymium or lanthanum trichloride failed. **2a-f** crystallize in the trigonal space group $P\bar{1}$,

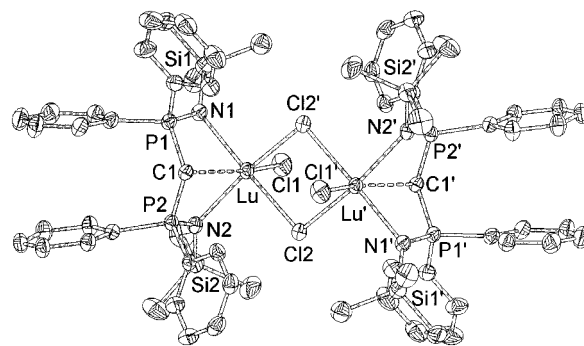


Figure 1. Perspective ORTEP view of the molecular structure of **2f**. Thermal ellipsoids are drawn to encompass 50% probability. Hydrogen atoms are omitted for clarity.

having one molecule of **2** and two molecules of toluene in the unit cell. **2a-f** are dimeric complexes in which the metal centers are bridged asymmetrically by two μ -chlorine atoms. In the center of the Ln-Cl₂-Ln'-Cl₂' plane, a crystallographic inversion center is observed. A comparison of the Ln-Cl₂-Ln' (102.00(1) $^\circ$ (**2e**) to 103.01(4) $^\circ$ (**2b**)) and Cl₂-Ln-Cl₂' angles (76.99(6) $^\circ$ (**2b**) to 78.00(5) $^\circ$ (**2e**)) of the central Ln-Cl-Ln'-Cl' four-membered ring of **2a-f** shows only a small influence of the center atom onto the observed geometry. The ligand geometry is as expected. The P-N and P-C bond distances as well as the P1-C1-P2 angles vary only slightly within the series **2a-f**. A six-membered metallacycle (N1-P1-C1-P2-N2-Ln) is formed by chelation of the two trimethylsilylimine groups to the lanthanide atom. The Ln-N distances as well as the Ln-Cl₁ bond length increase as expected with increasing ion radius of the center metal in a linear fashion. The ring adopts a twist-boat conformation in which the central carbon atom and the lanthanide atom are displaced from the N₂P₂ least-squares plane. The distance between the central carbon atom (C1) and the lanthanide atom (2.596(5) (**2f**) to 2.720(5) Å (**2b**)) is longer than usual Ln-C distances;¹ however the folding of the six-membered ring toward the lanthanide atom is caused by a weak interaction. The Ln-C1 bond lengths increase with increasing ion radius of the center metal in a linear fashion. The resultant tridentate coordination of the ligand was observed in **1**,²⁰ [Li(THF)]-[CH(PPh₂NSiMe₃)₂],²⁰ [Al(CH₃)₂{CH(PPh₂NSiMe₃)₂}],²⁶ [GaCl₂{CH(PPh₂NSiMe₃)₂}],²⁶ and [Ir{CH(PPh₂N(*p*-tolyl))₂}(COD)].²⁴ The Sm-C1 bond length of **2b** (2.720(5) Å) is significantly longer than that observed in the carbene-like complex [Cy₂NSm(THF){C(PPh₂NSiMe₃)₂}] (2.467(4) Å) (Cy = cyclohexyl).^{28d} This clearly indicates the difference in coordination chemistry of the monoanionic {CH(PPh₂NSiMe₃)₂}⁻ and the dianionic {C(PPh₂NSiMe₃)₂}²⁻ ligand. The endocyclic P-C bond distances (1.734(4)-1.761(5) Å) are significantly shortened compared to the exocyclic ones (1.808(4)-1.831(5) Å), suggesting that there is a considerable delocalization throughout the backbone of the ligand.

DFT Investigations. To rationalize and to better understand the nature of the Ln-C1 contacts, quantum chemical investigations of the asymmetric unit of **2a** were carried out at the density functional theory (DFT)²⁹ level (see Experimental Section). The calculations were undertaken by means of the program system Turbomole.³² The structure optimizations with the DFT

(40) Hultsch, K. C.; Voth, P.; Spanoil, T. P.; Okuda, J. *Organometallics* **2000**, *19*, 228-243.

(41) Kilimann, U.; Edelmann, F. T. J. *Organomet. Chem.* **1994**, *469*, C5-C9.

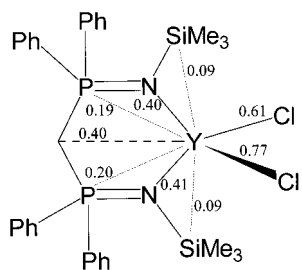


Figure 2. Schematic view of the calculated monomeric unit of **2a**. SEN values are denoted. Note that the latter only represent relative values, which have to be compared with SEN for reliable bonds in the same or in related structures. Selected bond lengths [Å] or angles [deg] (labeling corresponding to that given in Figure 1 or Table 2): Y–C1 2.726, Y–N1 2.318, Y–N2 2.323, Y–Cl1 2.537, Y–Cl2 2.538, P1–N1 1.645, P2–N2 1.645, P1–C1 1.769, P2–C1 1.767; Cl1–Y–Cl2 111.11, N1–Y–Cl1 101.81, N1–Y–Cl2 115.83, N2–Y–Cl1 101.62, N2–Y–Cl2 116.80, N1–Y–N2 107.74, P1–C1–P2 130.99, P1–N1–Y 101.79, P2–N2–Y 101.78.

method were followed by a population analysis based on occupation numbers after Ehrhardt and Ahlrichs.³⁸ Due to the reduction of a dimeric to a monomeric species (coordination number 5 instead of 6), the coordination sphere around the metal center was not perfectly reproduced regarding the bond angles. However, most of the calculated bond distances are in good agreement with the experimentally observed ones (maximum difference ca. 0.04 Å). One exception is one of the Y–Cl bonds, which can be due to differing steric as well as electronic situations due to differing coordination environments. Another exception is the Y–C1 contact, which is computed to be about 0.075 Å too long. This is, however, a typical result for the DFT investigations of a weaker or more dispersive interaction since DFT methods do not explicitly consider dispersion interactions. Therefore, we used the optimized monomeric structure to perform a population analysis. As a result, we present a shared electron number (SEN) of 0.40 for the Y–C contact that matches the values for the Y–N bonds in the monomer (SEN_{Y–N}: 0.40 and 0.41) and thus reveals the existence of a Y–C binding interaction. In contrast, SENs of the ones next to the neighbors, P or Si, amount to 0.19 and 0.20 (P) or 0.09 (Si), which shows the expected decrease. Figure 2 schematically shows the calculated molecule. Structural parameters are given in the caption; SEN values are denoted.

Lanthanide Amide Complexes. Transmetalation of the yttrium and the samarium chloro complex **2a** and **2b**, respectively, with an excess of KNPh₂ in toluene afforded the corresponding bisamido complexes [$\{\text{CH}(\text{PPh}_2\text{NSiMe}_3)_2\}\text{Ln}(\text{NPh}_2)_2$] (Ln = Y (**3a**), Sm (**3b**)) as crystalline solids (eq 2).³⁹ The new complexes have been characterized by standard analytical/spectroscopic techniques, and the solid-state structure of the yttrium compound was established by single-crystal X-ray diffraction (Figure 3). **3a** crystallizes in the trigonal space group $P\bar{1}$, having two molecules of **3a** and two molecules of toluene in the unit cell. Data collection parameters and selected bond lengths and angles are given in Tables 3 and 4. The structure reveals a distorted tetrahedral arrangement of the nitrogen atoms around the yttrium atom, having N–Y–N angles in the range of 101.90(10)° (N2–Y–N4) to 117.84(10)° (N1–Y–N3).

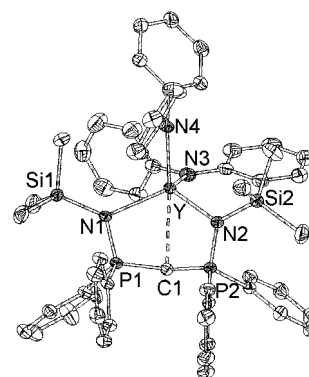
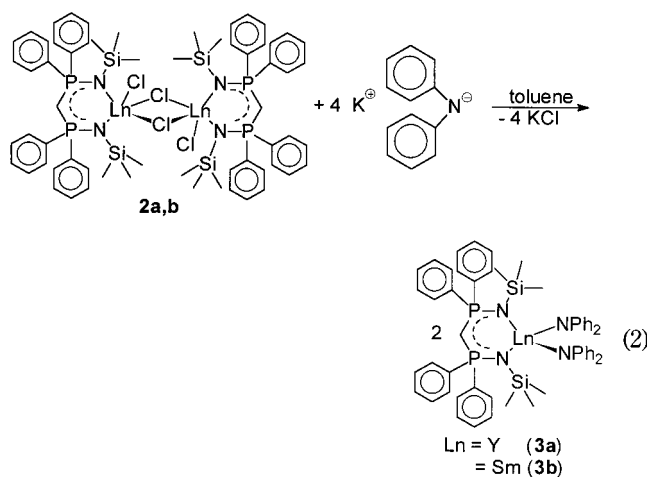


Figure 3. Perspective ORTEP view of the molecular structure of **3a**. Thermal ellipsoids are drawn to encompass 50% probability. Hydrogen atoms are omitted for clarity.

Table 4. Selected Bond Lengths (Å) and Angles (deg) of [$\{\text{CH}(\text{PPh}_2\text{NSiMe}_3)_2\}\text{Y}(\text{NPh}_2)_2$] (3a**)**

bond lengths (Å)		bond angles (deg)	
Y–C1	2.724(3)	N1–Y–N2	108.58(9)
Y–N1	2.348(2)	N1–Y–N3	117.84(10)
Y–N2	2.364(3)	N1–Y–N4	104.36(9)
Y–N3	2.250(3)	N2–Y–N3	117.29(10)
Y–N4	2.278(3)	N2–Y–N4	101.90(10)
P1–N1	1.615(2)	N3–Y–N4	104.63(10)
P2–N2	1.621(3)	P1–C1–P2	128.2(2)
P1–C1	1.746(3)	P1–N1–Y	101.14(12)
P2–C1	1.736(3)	P2–N2–Y	101.20(12)
P1–C2	1.817(3)	N1–Y–C1	64.64(9)
P2–C14	1.830(3)	N2–Y–C2	64.09(9)

The Y–N distance of the $\{\text{CH}(\text{PPh}_2\text{NSiMe}_3)_2\}^-$ ligand is about 0.1 Å longer (N1–Y 2.348(2) Å; N2–Y 2.364(3) Å) than the Y–NPh₂ bond length (Y–N3 2.250(3) Å; Y–N4 2.278(3) Å). Other yttrium complexes having comparable multidentate monoanionic ligands such as [$\{\text{(iPr)}_2\text{ATI}\}\text{Y}(\text{C}_5\text{Me}_5)_2$] (N–Y 2.398(2) and 2.390(3) Å)⁴² ($\{\text{(iPr)}_2\text{ATI} = N\text{-isopropyl-2-(isopropylamino)troponiminate}\}$) or [$\{\text{(Ph)N}=\text{C}(\text{Ph})\text{C}(\text{Ph})=\text{N}(\text{Ph})\}\text{Y}(\text{C}_5\text{Me}_5)_2$] (2.408–(4) Å)⁴³ feature similar bond lengths. The Y–NPh₂ distance is in agreement with other Y–N compounds, like the homoleptic amide $[\text{Y}\{\text{N}(\text{SiMe}_3)_3\}_3]$ ⁴⁴ (2.211(9) Å) and [$\{\text{tBu}(\text{Ar})_2\text{SiO}\}\text{Y}\{\text{N}(\text{SiMe}_3)_2\}_2$] (Ar = 2-C₆H₄(CH₂-NMe₂)) (2.237(9) Å).⁴⁵ As observed for **2a–f** a six-membered ring (N1–P1–C1–P2–N2–Y), which adopts a twist-boat conformation, is formed by the $\{\text{CH}(\text{PPh}_2\text{NSiMe}_3)_2\}^-$ ligand and the yttrium atom. The distance between the central carbon atom C1 and the yttrium atom (2.724(3) Å) is significantly longer than in **2a** (2.642(4) Å).



The multinuclear NMR data of **3** are consistent with the solid-state structure. The ^1H NMR spectrum of **3a** shows a downfield shift of the methine proton (δ 2.20) compared to the starting material **2a** (δ 1.93). In contrast to **2a** no $^2J(\text{H},\text{Y})$ coupling is seen. This effect might be caused by an increased Y–C bond length. Thus, the methine signal is split into a triplet, which is caused by a $^2J(\text{H},\text{P})$ coupling of 4.9 Hz. Complex **3a** shows a doublet in the $^{31}\text{P}\{^1\text{H}\}$ NMR spectrum (δ 22.1; $^2J(\text{P},\text{Y}) = 6.2$ Hz), which is in the same range as the one observed in **2a**. As a result of the paramagnetic influence of the samarium(III) atom, the NMR signals of **3b** are distributed over a wider range. Thus the resonance of the $\text{Si}(\text{CH}_3)_3$ group in the ^1H NMR spectrum is observed at δ -0.76 . The $^{31}\text{P}\{^1\text{H}\}$ NMR resonance of **3b** (δ 33.4) is, in comparison to $[\text{Cy}_2\text{NSm}(\text{THF})\{\text{C}(\text{PPh}_2\text{NSiMe}_3)_2\}]$ (δ 43.3), about 10 ppm upfield shifted.^{28d} In the EI mass spectra of **3a,b** the molecular ions as well as their characteristic fragmentation pattern were observed.

Summary

In summary, it can be emphasized that a series of lanthanide dichloride complexes having the monoan-

(42) Roesky, P. W. *Eur. J. Inorg. Chem.* **1998**, 593–596.

(43) Scholz, A.; Thiele, K.-H.; Scholz, J.; Weimann, R. *J. Organomet. Chem.* **1995**, 501, 195–200.

(44) Westerhausen, M.; Hartmann, M.; Pfitzner, A.; Schwarz, W. *Z. Anorg. Allg. Chem.* **1995**, 621, 837–850.

ionic $\{\text{CH}(\text{PPh}_2\text{NSiMe}_3)_2\}^-$ ligand in the coordination sphere were reported. These are the first lanthanide complexes having this ligand in the coordination sphere. The single-crystal X-ray structures of these complexes show that the methine carbon atom is bound to the lanthanide atom. This is supported by DFT calculations, which show a similar interaction. Due to the similar ion radii of the lanthanides, the single-crystal X-ray structures of **2a–f** are isostructural. The Ln–C_{methine} bond length increases linearly with increasing ion radius of the center metal. Further reaction of **2** with KNPh_2 led to new amide complexes. These complexes show in comparison to **2** a comparable coordination behavior of the $\{\text{CH}(\text{PPh}_2\text{NSiMe}_3)_2\}^-$ ligand in the solid state.

Acknowledgment. This work was supported by the Deutsche Forschungsgemeinschaft (Heisenberg fellowship) and the Fonds der Chemischen Industrie. Additionally, a lot of generous support from Prof. Dr. D. Fenske is gratefully acknowledged.

Supporting Information Available: X-ray crystallographic files in CIF format for the structure determinations of **2a–f** and **3a** are available free of charge via the Internet at <http://pubs.acs.org>.

OM0102955

(45) Shao, P.; Berg, D. J.; Bushnell, G. W. *Inorg. Chem.* **1994**, 33, 6334–6339.